PHYSICAL REVIEW B VOLUME 25, NUMBER 8 15 APRIL 1982

Electrical properties of neutron-transmutation-doped GaAs below 450 K

M. A. Vesaghi
Department of Physics and the James Franck Institute, The University of Chicago, Chicago, Illinois 60637
(Received 8 June 1981)

Various concentrations of Ge and Se donors were introduced into GaAs crystals by means of neutron transmutation doping. Three kinds of GaAs crystals were used: undoped, Cr-doped crystals, and a high-purity epitaxial layer. Hall coefficient R, resistivity ρ, and low-field magnetoresistance $\Delta\rho/\rho$ were measured between 1.4 and 450 K. Good agreement was found between the measured concentrations of added donors and the values expected from the neutron-capture cross sections and the neutron fluences used. The analysis of the temperature dependence of the carrier concentration of the epitaxial sample gave somewhat smaller values for N_D and N_A, the concentration of donors and acceptors, than the analysis of the T dependence of μ_H, but N_D-N_A was the same; this indicates that some deep-lying centers are present in this sample. At low T the magnetic field dependence of ρ of this sample was in good agreement with the theory of impurity conduction modified by Shklovskii. $\Delta\rho/\rho$ of this sample was positive to the lowest T (1.4 K) and had two peaks; one at about 50 K corresponds to a maximum of μ_H and the second one at about 4.2 K corresponds to the temperature at which band conduction and impurity conduction are of equal magnitude. At low T all the undoped and Cr-doped crystals had a negative magnetoresistance whose magnitude increases with decreasing T. At low T, $\Delta\rho/\rho$ changes from positive to negative as the room-temperature carrier concentration n_0 reaches 2×10^{15} cm^{-3}. Above this carrier concentration $\Delta\rho/\rho$ is negative and reaches a maximum value at $n_0\simeq1\times10^{16}$ cm^{-3}. $\Delta\rho/\rho$ disappears when n_0 exceeds the concentration of the true metallic state $n_{cb}\simeq5\times10^{17}$ cm^{-3}. The closeness of the n_0 value at which the negative $\Delta\rho/\rho$ has its maximum value and the critical concentration $N_c\simeq(3-4)\times10^{16}$ cm^{-3} at which the metal-nonmetal transition is observed indicates that these two phenomena are related.

I. INTRODUCTION

GaAs material is in great demand for high-frequency and high-speed GaAs devices such as Impatt diodes, Gunn diodes, field effect transistors, and avalanche photodiodes. The quality and control of impurities in GaAs material is much less advanced than in elemental semiconductors such as Si. This is partly because substitutional dopants can occupy either Ga sites or As sites and they tend to associate with defects and other impurities in the material. We have used a new method for preparing homogeneous and well-controlled GaAs material, namely neutron transmutation doping (NTD). This method was used for the first time by Cleland, Lark-Horovitz, and Pigg[1] thirty years ago. They showed that it is a convenient and highly reproducible method for introducing a homogeneous distribution of dopants into certain semiconductors. This work was continued by Fritzsche *et al.*,[2] Cuevas,[3] and others,[4] who made a detailed investigation of the electronic transport properties of transmutation-doped Ge. This method was applied to Te by Kuehnel *et al.*,[5] to InSb by Kuchar *et al.*,[6] and is now widely used in the manufacture of Si devices.

Besides a brief study by Mirianashvili *et al.*,[7] no detailed investigation of transmutation doping has been carried out on GaAs. This is quite surprising in view of the importance of GaAs as a device material, the difficulties encountered with regard to impurity and vacancy complexes, and the question whether Ge or other impurities are on Ga or As sites.

In the second section of this paper the theory of NTD in GaAs is discussed; Sec. II A is on NTD processes and the number of dopants, and it is followed by a section on damages due to the recoils

of γ and β particles produced by the NTD processes. In Sec. III the experimental details are discussed. Undoped (not intentionally doped) and Cr-doped (semi-insulating) melt-grown GaAs crystals as well as one epitaxially grown (pure) GaAs crystal were exposed to various fluxes of thermal neutrons. The data of Hall effect R and resistivity ρ measurement between 450 and 1.4 K for undoped and Cr-doped samples are given in Sec. IV A. In Sec. IV B a two-band model which is used to estimate the compensation ratio is discussed. The R and ρ data for the epitaxial sample are given in Sec. IV C. Section IV D presents magnetoresistance measurements on all samples. The metal-to-nonmetal transition (M-NM) and its relation to the magnetoresistance is discussed in Sec. V. The last section presents a summary and our conclusion. Part of the data of Sec. IV A were reported in a previous paper.[8]

II. THEORY OF NTD IN GaAs

A. NTD process and the density of dopants

Introducing dopants into GaAs by the way of transmutation is done as follows. Thermal neutrons are captured by various nuclei in GaAs in proportion to the relative abundance of Ga and As isotopes and their capture cross section. After a neutron is captured by, for instance, an ^{75}As nucleus, an ^{76}As nucleus is formed which is in an excited state. This excited nucleus decays quickly to its ground state by emitting a photon

$$^{75}\mathrm{As}+n\rightarrow{}^{76}\mathrm{As}+\gamma\ . \tag{1}$$

This new ^{76}As nucleus is, however, not stable. It decays into a ^{76}Se nucleus by β particle emission.

$$^{76}\mathrm{As}\rightarrow{}^{76}\mathrm{Se}+\beta^-\ . \tag{2}$$

All naturally occurring isotopes of Ga and As participate in transmutation doping with the following reactions[9]:

$$^{69}\mathrm{Ga}(n,\gamma)^{70}\mathrm{Ga}\rightarrow{}^{70}\mathrm{Ge}+\beta^-\ \ (21\ \mathrm{min})\ , \tag{3}$$

$$^{71}\mathrm{Ga}(n,\gamma)^{72}\mathrm{Ga}\rightarrow{}^{72}\mathrm{Ge}+\beta^-\ \ (14\ \mathrm{h})\ , \tag{4}$$

$$^{75}\mathrm{As}(n,\gamma)^{76}\mathrm{As}\rightarrow{}^{76}\mathrm{Se}+\beta^-\ \ (26\ \mathrm{h})\ . \tag{5}$$

The numbers in parentheses are half-lives for the β decays. If the resultant Ge atoms are found at Ga sites and the Se atoms at As sites, one expects that all end products will act as donors.

The density of transmutation donors n_{NTD} due to the capture of thermal neutrons follows from

$$n_{\mathrm{NTD}}=\Phi\sum_i n_i\sigma_c^i\ , \tag{6}$$

where $\Phi=\phi t$ is the thermal neutron fluence (flux$\times$time), n_i is the concentration of ith isotope, and σ_c^i is its capture cross section.

If the capture cross section increases with the inverse of the neutron velocity, then one obtains

$$\sigma_c=(\sqrt{\pi}/2)\sqrt{300/T}\,\sigma_c(V_0)\ , \tag{7}$$

where $V_0=2200$ m/s is the most probable neutron velocity at 300 K and T is the effective neutron temperature. Combining Eqs. (6) and (7) yields

$$n_{\mathrm{NTD}}=(\sqrt{\pi}/2)\sqrt{300/T}\sum_i n_i\sigma_c^i(V_0)\ . \tag{8}$$

Until now we have only considered thermal neutrons. The neutrons in a reactor cannot be described simply by a thermal spectrum; they have a wide energy spread $\phi(E)$ extending from 1 to 10 MeV. Thus, in addition to thermal neutrons, we should consider neutron absorption due to the resonance capture which takes place in the epithermal part of the neutron flux. Contributions from the high-energy region (above the epithermal part) are, however, negligible since neutron-capture cross sections in general decrease as $1/V$. Therefore, the cross sections for higher-energy neutrons are a few orders of magnitude smaller than those in the thermal region. Furthermore, the nonthermal neutron density is very small at the places in the reactor chosen for the irradiation.

Finally, when all types of (n,γ) reactions are included the transmutation, donor density can be expressed by

$$n_{\mathrm{NTD}}=\Phi\sum_i n_i[A\sigma_c^i(V_0)+BI^i]\ , \tag{9}$$

where $B=2\times10^{-2}$ is the ratio of the epithermal to the thermal flux of neutrons per unit lethargy (the logarithmic interval of the energy), I^i is the resonance integral for ith isotope,[10] and $A=(\sqrt{\pi}/2)\times(300/T)^{1/2}$. The values of n_i, σ^i, and I^i for Ga and As isotopes are listed in Table I.

From the values listed in Table I and Eq. (9) we obtain

$$n_{\mathrm{NTD}}=\Phi(2.435/\sqrt{T}+0.036)\ . \tag{10}$$

Unfortunately, after the transmutation reactions (3)–(5) the transmuted atoms are usually not in their original positions but displaced into interstitial positions due to the recoil produced by the γ

and β particles in the nuclear reactions. Part of this study is to see whether the transmuted atoms can be returned to their original positions and radiation damages can be healed by annealing the samples.

B. Damage and annealing

After the GaAs samples have been irradiated in the reactor and the induced radioactivity has been allowed to decay, the samples are found to have very low carrier concentrations and very high resistivities. This is due to deep-lying defect levels which are produced during transmutation doping. The causes for these defects are (i) fast neutron knock-on displacements, (ii) gamma recoil, (iii) beta recoil. Damage due to the fast neutrons is discussed by many authors[11] and so will not be discussed here. The recoil energies from the γ and β emissions are

$$E_R(\gamma)=E_\gamma^2/2Mc^2 , \tag{11}$$

$$E_R(\beta)=E_\beta(E_\beta+2mc^2)/2Mc^2 , \tag{12}$$

where M is the mass of the recoiling nucleus, m is the electron rest mass, and E_γ and E_β are the energies of γ and β particles, respectively.

The recoil energies due to the γ emission cover a range of values because various decay channels are possible. Decay with the highest γ energy $E_\gamma \simeq 7.5$ MeV occurs with low probability (1%).[12] The most probable decay proceeds by emission of two or three photons of lower energies. Table II lists the recoil energies involving one, two, and three photons, respectively.

The range of recoil energies associated with β decay depends on the correlation between the emitted neutrino and the β particle. We also list in Table II the maximum $E_R(\beta_{\max})$ and most probable values $E_R(\beta)$ of the β recoil energy.

Since only 9 and 10 eV are required for the creation of Frenkel defects in the Ga and in the As sublattices of GaAs, respectively,[13] one finds that the number of defects due to the beta and gamma recoils as well as to fast neutron knock-on displacements is very large indeed. This agrees with our finding that the samples have a very high resistivity and very low carrier concentrations after irradiation.

For removing these damages high-temperature annealing was needed: 800 °C for melt-grown crystals and 600 °C for the epitaxial one. The higher anneal temperature required for melt-grown crystals is presumably associated with their higher concentration of defects and impurities, which act as binding sites for the transmuted atoms or the recoil defects.

III. EXPERIMENTAL DETAILS

Undoped and Cr-doped (semi-insulating) melt-grown crystals were purchased from Laser Diode Lab. Inc. Bridge-shaped samples with three electrode arms on one side and one electrode arm on the other side having enlarged pads for current contact were ultrasonically cut from 0.1 cm-thick wafers. Both undoped and Cr-doped samples were etched in $1H_2O$, $5H_2SO_4$, $1H_2O_2$ solution. Ohmic contacts were made by alloying small balls of Ge-Au to the samples at 450 °C. The contacts were removed before irradiation and annealing and attached for electrical measurements. The undoped crystals contained an excess electron concentration of about 3×10^{16} cm^{-3} with the exception of one sample which had 5×10^{16} cm^{-3}. The Cr-doped crystals had a room-temperature resistivity larger than 10^7 ohm cm. The epitaxially grown crystal[14] was a square platelet with dimensions $0.5\times0.5\times0.02$ cm^3. This sample contained 2.1×10^{14} cm^{-3} donors and 5.7×10^{13} cm^{-3} acceptors.

The samples were irradiated at the Research

TABLE I. Concentration, capture cross section, and resonance integral for Ga and As isotopes.

Isotope	n (10^{22} cm^{-3})	σ_c^i (barn)	I^i (barn)
^{69}Ga	1.332	1.68±0.07[a]	15.6 ±1.5[a]
^{71}Ga	0.881	4.86±0.28[a]	31.2±1.9[a]
^{75}As	2.213	4.3±0.1[a]	60±4[a]

[a]Reference 10.

TABLE II. Recoil energies in eV.

Isotope	E_R (1γ)	E_R (2γ)	E_R (3γ)	E_R (β_{max})	E_R (β)
^{70}Ga	457	228	152	33	16
^{72}Ga	444	222	148	100	50
^{76}As	375	187	125	83	41

Reactor Facility of the University of Missouri in a thermal neutron flux of $\phi = 5 \times 10^{11}$ n/cm^2 sec. The actual thermal neutron temperature was about 30° higher than room temperature. The total neutron dose (fluence) was measured by rhodium wire with a maximum error of 5% in Φ. Annealing of the melt-grown samples was carried out at 800 °C in an inert-gas atmosphere after a pyrolytic Si_3N_4 encapsulation to prevent As evaporation. The epitaxial layer was also annealed at 600 °C for 1 h in an inert gas atmosphere.

IV. RESULTS AND DISCUSSION

A. Undoped and Cr-doped samples

Table III lists the Hall coefficient R, resistivity ρ, as well as the electron density $n = 1/Re$, and the Hall mobility $\mu_H = R/\rho$ measured at 300 K before and after transmutation doping for the undoped melt-grown GaAs. The unirradiated sample No. 0 is included in Table III for testing the quality of the Si_3N_4 encapsulation. This sample was measured before and after annealing at 800 °C for 10.5 h. It is known that As atoms evaporate at temperatures higher than 650 °C and produce vacancy-donor complexes.[15] These are expected to result in a reduction in n and μ_H. Instead we observe a small increase in carrier concentration and an improvement in mobility. It appears that annealing removes some low-lying acceptor states or deep electron traps which were initially present in the material, but no effects of As evaporation were observed. Since the Hall factor $r = nRe$ is larger than one for an isotropic band such as the conduction band of GaAs,[16] the carrier concentrations n given in Table III are underestimated. Measurement at

TABLE III. Characteristics at 300 K of undoped GaAs samples before and after transmutation doping.

	Sample no.	0	1	2	3	4	5
Before irradiation	R (cm^3/C)	263	216	111	254	249	245
	ρ (ohm cm)	0.07	0.06	0.029	0.072	0.07	0.068
	n (10^{16} cm^{-3})	2.37	2.89	5.64	2.46	2.5	2.55
	μ_H (10^3 cm^2/V s)	3.78	3.6	3.8	3.53	3.56	3.6
Φ (10^{17} n/cm^2)		0	1.0	1.0	2.0	9.37	18.75
Anneal time (h)		10.5	5	12.5	10.5	4.5	4.5
After irradiation and annealing	R (cm^3/C)	193	131	78.9	101	37.5	19.2
	ρ (ohm cm)	0.04	0.035	0.021	0.024	0.0094	0.0055
	n (10^{16} cm^{-3})	3.23	4.75	7.91	6.2	16.7	32.5
	μ_H (10^3 cm^2/V s)	4.35	3.71	3.8	4.19	3.97	3.47
	Δn (10^{16} cm^{-3})	0.86	1.86	2.27	3.74	14.2	30
	n_{NTD} (10^{16} cm^{-3})	0	1.72±0.15	1.72±0.15	3.44±0.27	16.1±1.4	32.1±2.7

450 K indicated that considering the carrier density at 300 K as the excess electron concentration would be an underestimation by less than 10% due to the carrier freeze-out. The last two rows in Table III compare the measured change in carrier concentration Δn with that expected from Eq. (10), using the irradiation fluences Φ listed in row 5. The errors in the last row were calculated from the errors in fluences and the errors in capture cross sections. By considering the increase in carrier concentration because of the annealing alone and the underestimation due to the carrier freeze-out at 300 K and due to using Hall factor $r=1$, we find the close agreement between the measured and calculated values of the donor concentration introduced by transmutation doping very satisfactory. This shows that indeed most Ge atoms are on Ga sites and most Se atoms are on As sites after annealing. Intersite defects are expected to act as acceptors; the agreement between Δn and n_{NTD} indicates that fewer than 5% transmuted atoms form intersite defects. Table IV lists the values of R, ρ, μ_H, and n measured at 300 K after the irradiation and annealing for the Cr-doped melt-grown samples, and in addition, n_{NTD} for each sample. Annealing was carried out at 800 °C for 4.5 h.

The efficiency of transmutation doping in Cr-doped GaAs cannot be assessed by comparing the last two rows of Table IV. This is because these samples are compensated and therefore the compensation ratio $K=N_A/N_D$ must be determined before one can obtain N_D from the measured $n_0=N_D-N_A$. K cannot be determined by using ordinary analysis of the temperature dependence of carrier concentration because the change in Hall coefficient and, hence, in carrier concentration n due to the temperature change is small (see Fig. 2). In the next section we will use a two-band model for estimating K. Figures 1 and 2 show the temperature dependence of ρ and R, respectively, for the samples listed in Tables III and IV. The nonirradiated sample before annealing is denoted by (00) and after annealing by (0). The resistivity curves show two activation regimes. The larger activation energy E_1 at high temperature is due to excitation of carriers into the conduction band. The smaller low-temperature activation energy E_2 which goes to zero as the carrier concentration n reaches 3×10^{16} cm^{-3}, is associated with the impurity-band conduction. The maximum in the Hall curves near 80 K is due to the transition from band conduction to impurity conduction. This will be discussed in the next section.

B. Two-band conduction

When the impurity levels are separated in energy from the conduction band, the conduction-band carriers freeze out into the impurity levels as the temperature is lowered. Since R is inversely proportional to the carrier density, we expect R to increase with decreasing temperature. Our results as well as those of other groups[17–24] on GaAs show that R does not rise indefinitely but goes through a maximum as the temperature is decreased. The same behavior has been observed in Ge,[25] InSb,[26] InP,[24] and other semiconductors. At low temperatures the conduction process is dominated by phonon-assisted hopping of electrons among the impurity levels. The Hall maximum occurs at the temperature where band conduction and impurity conduction are of comparable magnitude. The expression for σ and R for two-band conduction are[27]

$$\sigma=e(n_c\mu_c+n_i\mu_i) \tag{13}$$

$$R=\frac{1}{e}(n_c\mu_c^2+n_i\mu_i^2)/(n_c\mu_c+n_i\mu_i)^2 , \tag{14}$$

TABLE IV. Characteristics at 300 K of Cr-doped GaAs samples after transmutation doping.

Sample no.	1C	2C	3C	4C
R (cm^3/C)	560	323	111	40.2
ρ (ohm cm)	0.235	0.143	0.043	0.014
μ_H (10^3 cm^2/V s)	2.38	2.25	2.56	2.97
n (10^{16} cm^{-3})	1.1	1.72	5.63	15.5
n_{NTD} (10^{16} cm^{-3})	8.0±0.7	9.65±0.8	16.1±1.4	32.2±2.7

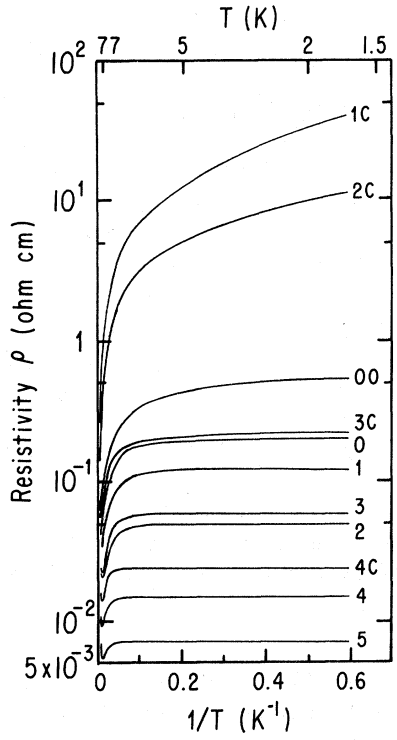

FIG. 1. Temperature dependence of the resistivity of GaAs samples. The characteristics of these samples are listed in Tables III and IV.

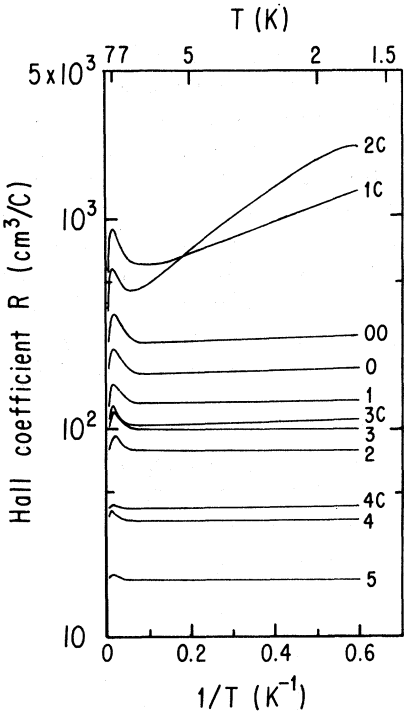

FIG. 2. Temperature dependence of the Hall coefficient of the samples of Fig. 1.

where n_c and μ_c are the concentration and the mobility of the carriers in the conduction band and n_i and μ_i are the corresponding values of the carriers moving between the impurities.

The total electron density for n-type material in the extrinsic region is

$$n_0 = N_D - N_A = n_c + n_i \ . \tag{15}$$

Now Eq. (14) can be written as

$$R = (1/n_0 e)\frac{[x(b^2-1)+1]}{[x(b-1)+1]^2} \ , \tag{16}$$

with $b = \mu_c/\mu_i$ and $x = n_c/n_0$. Since b changes slowly with temperature compared to n_c, R in Eq. (16) will have a maximum at $x = 1/(b+1)$. This occurs when impurity conduction is equal to the band conduction. One can obtain the value of b from Eq. (16) and the condition for the Hall maximum

$$(R_{\max}/R_{\text{exh}}) = (b+1)^2/4b \ , \tag{17}$$

where $R_{\max}$ is the value of R at its maximum and $R_{\text{exh}} = 1/n_0 e$ is the value of R in the exhaustion range where all donors are ionized. Using the value of b obtained from Eq. (17), the exhaustion electron concentration n_0, and the measured Hall coefficient at a given temperature, one can calculate x from Eq. (16) and hence the electron concentration $n_c = x n_0$ at that temperature. The calculation of n_c becomes impossible only at the lowest temperatures where the Hall coefficient becomes constant or as in sample 1*C*, 2*C*, and 3*C* for which R increases after reaching a minimum as T is lowered. Figure 3 shows the temperature dependence of $n = 1/Re$, n_c, and $n_i = n_0 - n_c$ which are calculated by this model for samples 4 and 2*c*. R and n at room temperature were considered as R_{exh} and n_0, respectively. The curves show the typical behavior of the n, n_c, and n_i for two simultaneous conduction processes.

We now turn to the problem of determining the compensation ratio of the melt-grown crystals. Analysis of the temperature dependence of the Fermi level E_F provides a method for the simultaneous determination of the impurity activation energy E_1, the donors concentration N_D, and the compensation ratio $K = N_A/N_D$. If we assume that the number of impurity levels is equal to $2N_D$ due to the lifting of the spin degeneracy and if the distribution of the impurity levels is narrow, then with $E = 0$ at the conduction-band edge[20]:

$$n_i = \frac{2N_D}{1+\exp[(-E_1 - E_F)/kT]} \ . \tag{18}$$

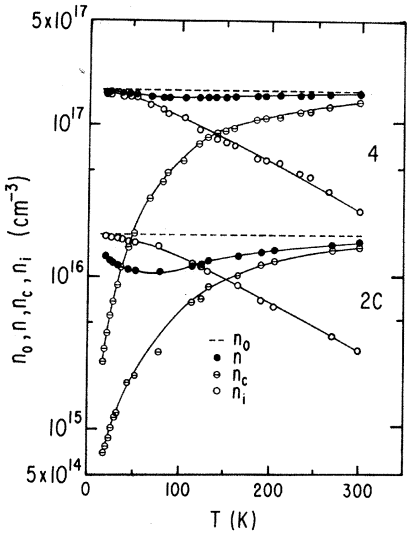

FIG. 3. Temperature dependence of $n=1/Re$, concentration of carriers in conduction band n_c, concentration of carriers in the impurity band n_i, and carrier concentration at 300 K, n_0 of samples 4 and 2C.

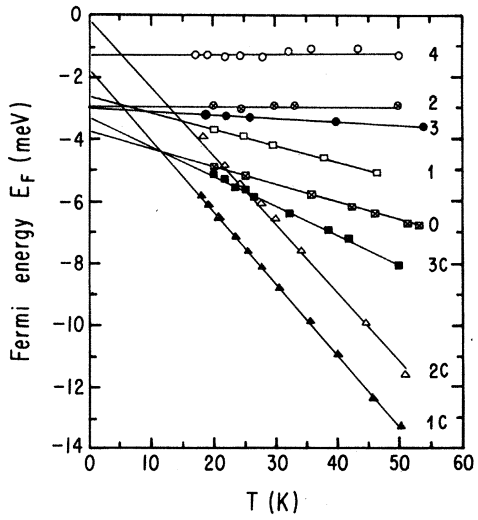

FIG. 4. Fermi energy as a function of absolute temperature of some of the samples listed in Tables III and IV.

Hence,

$$E_F=-E_1-kT\ln\left[\frac{2N_D}{n_0-n_c}-1\right]. \tag{19}$$

When $n_c<<n_0$, the temperature region below the temperature of the Hall-coefficient maximum, the temperature dependence of E_F is a straight line which intersects the ordinate at the point $E_F=-E_1$ and whose slope $-\ln[2N_D/(n_0-n_c)-1]\simeq-\ln[(1+K)/(1-K)]$ is determined by the degree of compensation $K=N_A/N_D$.

Knowing n_c at any temperature, E_F can be determined from the usual formula for a parabolic conduction band:

$$n_c=N_cF_{1/2}(\tilde{E}_F)\,, \tag{20}$$

where the functions $F_{1/2}(\tilde{E}_F)$ are tabulated Fermi integrals (Ref. 28), $\tilde{E}_F=E_F/kT$, and N_c is the effective conduction-band density of states. Figure 4 gives the temperature dependence of E_F; for $N_D<1.7\times10^{17}$ the dependence of E_F on T is linear with zero or negative slope which is the characteristic of a narrow impurity band.[26] E_1, N_D, and K, which were determined from the intercepts and the slopes of the lines in Fig. 4, are listed in Table V.

It is evident from this table that the activation energy E_1 decreases with increasing N_D. A comparison of different samples shows that E_1 depends not only on N_D, but also on N_A or K. The last row in Table V shows that the compensation in Cr-doped samples is very large and, unfortunately, the density of acceptors is varying from sample to sample. Hence, it is difficult to do a systematic and quantitative study of transmutation doping in Cr-doped samples. The analysis of E_F is based on the assumption that the impurity band is narrow

TABLE V. Activation energy E_1, donor concentration N_D, and compensation ratio K, calculated by using two-band model.

Sample no.	0	1	2	3	4	1C	2C	3C
E_1 (meV)	3.7	2.6	2.9	3	1.2	1.7	0.15	3.2
N_D (10^{16} cm^{-3})	5	7	8	6.7	17.3	8.5	13	12.5
$K=N_A/N_D$	0.3	0.3	~0	0.06	~0	0.87	0.85	0.52

and separated from the conduction band. As is discussed by Fritzsche,[29] this assumption becomes a serious problem at carrier concentration above the M-NM transition density N_c. All our melt-grown samples have carrier densities near or above N_c; therefore, one should not take the number listed in Table V too seriously.

C. Expitaxial sample

The thermal neutron fluence for this sample was 7.5×10^{15} n/cm^2, which corresponds to an expected $n_{NTD}=1.27\times10^{15}$ cm^{-3}. Figure 5 shows the temperature dependence of R and ρ for the epitaxial sample. R has a maximum at about 4.2 K; the slope of ρ changes at about the same temperature. This again is the transition temperature between dominant band conduction at higher temperatures and impurity conduction at lower temperatures. At low temperatures this sample has an activated resistivity. For phonon-assisted hopping between donor sites we can write[25]

$$\rho=\rho_3\exp(E_3/kT) . \tag{21}$$

Calculated values of ρ_3 and E_3 from the experimental curve are given in Table VI. These values are close to the reported values for samples similar to ours by Halbo and Sladek[30] and by Kahlert and Landwehr.[31]

Figure 6 gives the temperature dependence of $n=1/Re$ for the epitaxial sample. The curve was obtained by fitting the measured carrier concentration to the following expression:

$$\frac{n(N_A+n)}{(N_D-N_A-n)}=\frac{N_c}{2}\exp(E_D/kT) . \tag{22}$$

E_D is the ionization energy of the donor impurities. The values of N_D, N_A, and E_D which give

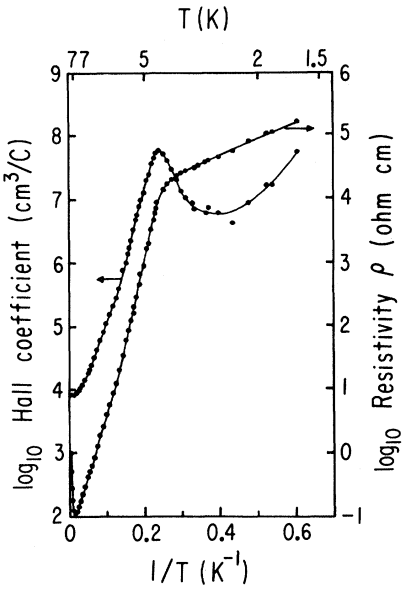

FIG. 5. Temperature dependence of the Hall coefficient and the resisitivity of the epitaxial sample.

the best fit are listed in Table VI. Deviation of the data from the calculated curve at low temperatures is due to the transition from band conduction to impurity conduction. The small dip in measured carrier concentration between 77 and 300 K is caused by the temperature dependence of the Hall factor r for polar optical-phonon scattering.[32]

Figure 7 shows the temperature dependence of Hall mobility μ_H of the epitaxial sample. The sharp decrease below 6 K is again due to the transition from band conduction to impurity conduction. The mobility curve was calculated by using a combination of scattering by polar optical phonons, piezoelectric acoustic phonons, deformation-potential acoustic phonons, ionized impurities, and neutral impurities in the relaxation time.[33] At the temperatures between 6 and 60 K the dominant

TABLE VI. Characteristics of epitaxial sample.

ρ_3 (ohm cm)	E_3 (meV)	E_D (meV)	N_D (10^{14} cm^{-3})	N_A (10^{14} cm^{-3})
4500	0.51	4.7[a]	8.6[a]	0.2[a]
			9.8[b]	1.4[b]

[a]Analyzing T dependence of n.
[b]Analyzing T dependence of μ_H.

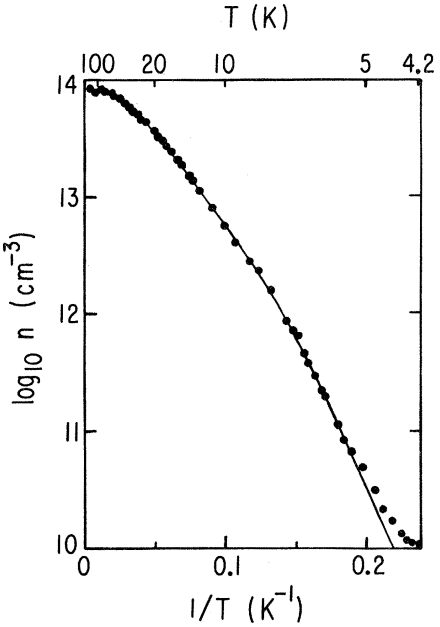

FIG. 6. Carrier concentration n as a function of $1/T$ of epitaxial sample. Solid curve is the best fit of Eq. (22) of text to the experimental data.

scattering processes are those from ionized impurities and neutral impurities. Between 60 and 90 K scattering by piezoelectric and acoustic phonons have some effect on the mobility, and at temperatures above 90 K the dominant process is polar optical-phonon scattering. The method of analyzing polar optical-phonon scattering failed completely between about 120 to 300 K.[33] Because of this the calculated mobility was not extended above 120 K. The values of N_D and N_A which best fit the experimental data are also given in Table VI. These values are somewhat larger than those obtained by analyzing the temperature dependence of carrier density. However, the value of $N_D - N_A$ is the same. This indicates that there are some deep donor and acceptor centers which act as ionized impurity centers for scattering but do not contribute to the carrier density.

On the other hand, the values of N_D and N_A which were calculated by using the Wolf master curve[34] of the mobility at 77 K and which were reported by us earlier,[8] were too large. This is because Wolfe's method does not include the effect of the deep impurities on the mobility.

D. Magnetoresistance

Figure 8 shows the field dependence of the magnetoresistance $\Delta\rho/\rho$ at 4.2 K and 2.5 K for some of the samples listed in Table III and IV. At low temperatures $\Delta\rho/\rho$ of all samples is negative up to the highest magnetic field used. The magnitude of $\Delta\rho/\rho$ increases with decreasing temperature. Following Zavaritskaya *et al.*[35] we assume that the magnetoresistance may be decomposed in two components:

$$\Delta\rho/\rho=(\Delta\rho/\rho)_- +(\Delta\rho/\rho)_+ , \tag{23}$$

where the second term is the usual magnetoresistance due to the difference in the Lorentz forces for carriers with different velocities. It is proportional to B^2. The first term $(\Delta\rho/\rho)_-$ is believed to be due to the localized spin alignment in the magnetic field and can be written as follows[30,35]:

$$(\Delta\rho/\rho)_- \sim -(B/T+\theta)^2 , \quad B\to 0 \tag{24}$$

$$(\Delta\rho/\rho)_- \to \text{const}, \quad B\to\infty . \tag{25}$$

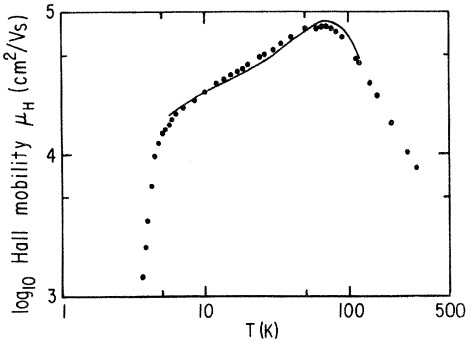

FIG. 7. Temperature dependence of the Hall mobility of the sample of Fig. 6. Solid curve is the calculated combined mobility (see text).

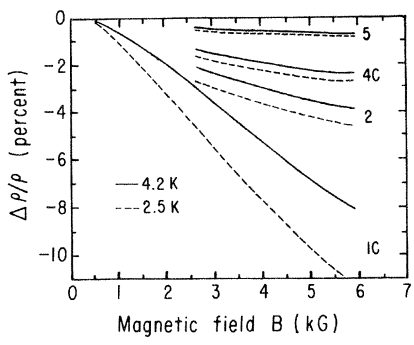

FIG. 8. Magnetic field dependence of the magnetoresistance of some of the samples listed in Tables III and IV at 4.2 and 2.5 K.

TABLE VII. θ and b were deduced from negative magnetoresistance data.

Sample no.	1C	3C
θ (K)	5.5	5.8
b (10^{-3} kG^{-2})	5.3	4.8

Thus, for low magnetic field we have

$$\Delta\rho/\rho=-(B/T+\theta)^2+bB^2 , \quad (26)$$

where b and θ are constants which have different values for each sample. The values of θ and b which were deduced from the data of samples 1C and 3C using Eq. (26) are listed in Table VII. These values of θ and b are about three times larger than those reported by Halbo and Sladek[30] for their samples, which have a donor concentration of about a factor of 10 smaller than our samples.

The epitaxial sample with carrier concentration about 8.2×10^{14} cm^{-3} at 300 K has a positive magnetoresistance in the whole temperature range investigated, as shown in Fig. 9. At high T in the band conduction range the field dependence of $\Delta\rho/\rho$ is quadratic at low fields and becomes close to linear at high field. In the impurity conduction range at low T the magnetoresistance is proportional to B^2. According to the theory of the weak-field magnetoresistance for impurity conduction which was modified by Shklovskii[36] to include the results of percolation theory, the magnetic field dependence of the resistivity can be written as

$$\rho(B)=\rho(0)\exp(ta^{*}B^2e^2/N_Dc^2\hbar^2) , \quad (27)$$

where a^* is the effective Bohr radius of impurity atoms and t is a constant. This theory predicts that the logarithmic derivative of $\rho(B)$ with respect to B^2 is independent of temperature. Our data shown in Fig. 10 is in good agreement with this prediction. We obtain $t=0.039$ which is very close to the theoretical value[37] $t=0.04$.

Figure 11 shows the temperature dependence of magnetoresistance at 5 kG. Starting at high temperature, the magnetoresistance increases with decreasing temperature, reaches a maximum at about 50 K, and then decreases. This temperature dependence is very similar to that of the mobility (Fig. 7). This is expected, since for band conduction $\Delta\rho/\rho$ is a function of (μB). The second maximum occurs at about 4.2 K where the Hall coefficient has a maximum due to the transition from band conduction to impurity conduction. In the transition region the excess electron n_0 is divided into

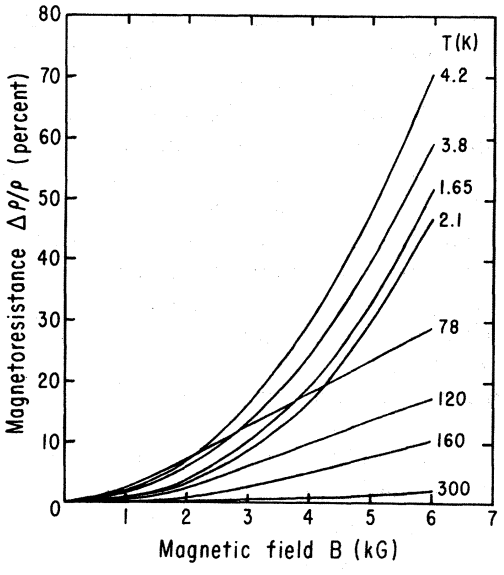

FIG. 9. Magnetic field dependence of the magnetoresistance of the epitaxial sample at different temperatures.

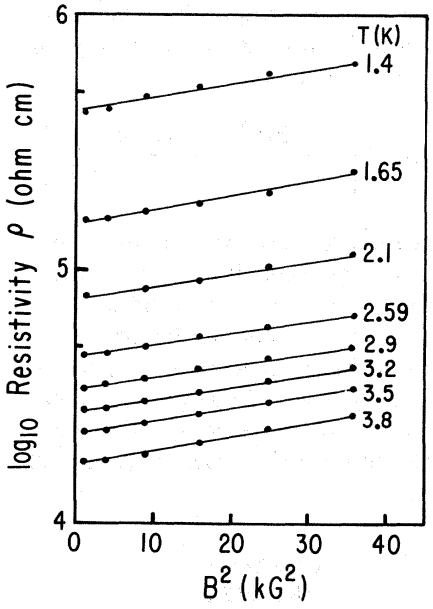

FIG. 10. Resistivity as a function of the square of the magnetic field at temperatures below 4.2 K of the sample of Fig. 9.

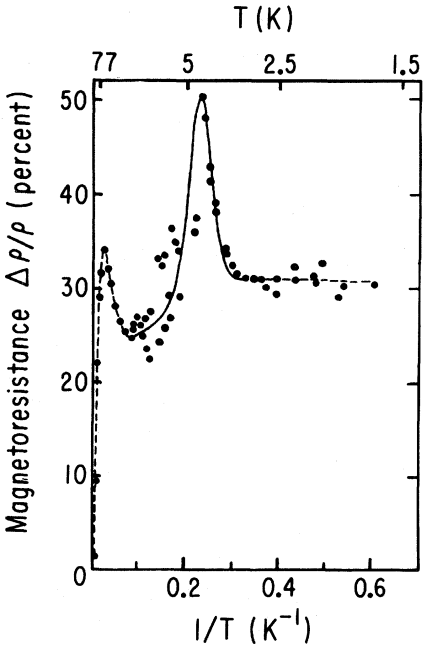

FIG. 11. Temperature dependence of the magnetoresistance at 5 kG of the epitaxial sample. Solid curve is the magnetoresistance calculated by the method described at the end of Sec. IV D.

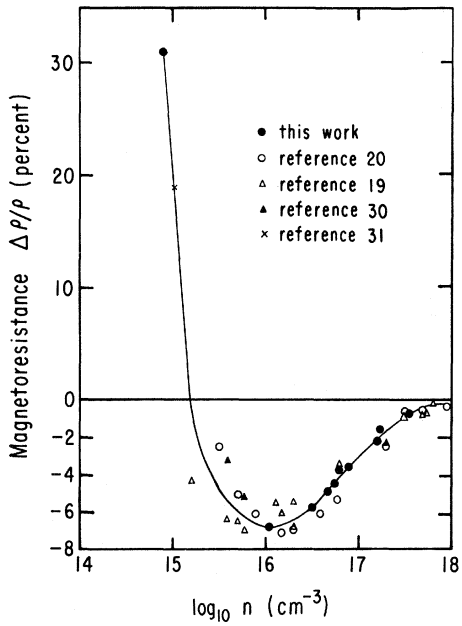

FIG. 12. Magnetoresistance at 5 kG and 4.2 K as a function of carrier concentration at 300 K of our samples and those of other authors.

two parts, one part in the conduction band with one average velocity, the other part in the impurity band with different average velocity. In a magnetic field this velocity difference causes a magnetoresistance which is in addition to the magnetoresistance for two bands. This magnetoresistance, which is important in the transition region, can be written as follows[38]:

$$\frac{\Delta\rho}{\rho}=(\mu_i B)^2\left[\frac{\sigma_c+\sigma_i b^2}{\sigma_c+\sigma_i}-\left[\frac{\sigma_c+\sigma_i b}{\sigma_c+\sigma_i}\right]^2\right]. \quad (28)$$

This equation reaches a maximum when $\sigma_c=\sigma_i$, which is the same condition as for the maximum of the Hall coefficient. The solid curve in Fig. 11 was computed by assuming that above 10 K, $\Delta\rho/\rho$ is due to the band conduction only; below 3 K, $\Delta\rho/\rho$ is solely due to the impurity conduction and a linear transition in between, and by adding to this magnetoresistance $\Delta\rho/\rho$ of the Eq. (28).

V. MAGNETORESISTANCE NEAR THE METAL-NONMETAL TRANSITION

The magnetoresistance of GaAs measured at 5 kG and 4.2 K is plotted against the room-temperature carrier density in Fig. 12. Besides our own data we included the results of several other authors. As discussed in the previous section, the large positive $\Delta\rho/\rho$ at small n is due to the shrinkage of the donor wave functions perpendicular to B. According to Eq. (27) this effect decreases with increasing N_D and hence with n. The observed decrease is, however, more rapid than expected from Eq. (27) because this equation ceases to be valid as the overlap of the donor wave functions becomes stronger. The magnetoresistance becomes negative for $n>1.5\times10^{15}$ cm^{-3}. The magnitude of this negative $\Delta\rho/\rho$ reaches a maximum near $n=10^{16}$ cm^{-3} and then decreases as n is increased to 10^{18} cm^{-3}. This negative magnetoresistance is attributed to an interaction of free or semifree carriers in the impurity band with magnetic moments of localized spins.[35,39] We conclude from Fig. 12 that the formation of the impurity band begins near $n=2\times10^{15}$ cm^{-3} and that it has essentially merged with the conduction band near 5×10^{17} cm^{-3}.

According to Mott's criterion[40] the metal-nonmetal transition occurs at a critical concentration N_c of the majority impurities

$$N_c=0.018/(a^*)^3, \quad (29)$$

independent of compensation. This yields $N_c=2.3\times10^{16}$ cm^{-3} with $a^*=92$ Å for n-type

GaAs. In the following we compare our observations with Mott's criterion and the concentration of the maximum of the negative magnetoresistance with a model of Shmatrsev.[39] He has shown that the formation of localized spins requires fluctuations on a scale $r_1 > a_B, r_D$, meaning that if an impurity center is separated from its nearest neighbors by a distance $r > r_1$, the electron in that center will be localized; in this model it is assumed that the impurities are distributed randomly in accordance with the Poisson equation. With this assumption the density of localized magnetic moments, i.e., localized spins, is

$$N_m = N \exp(-\tfrac{4}{3}\pi N r_1^3) , \tag{30}$$

where N is the total density of the impurities which is equal to electron concentration for noncompensated material. N_m is maximum when $\frac{4}{3}\pi N r_1^3$ is equal to one. From Fig. 12 we see that the maximum of negative magnetoresistance occurs when the carrier concentration lies between 1×10^{16} cm^{-3} and 2×10^{16} cm^{-3}, which for undoped GaAs gives

$$r_1 = (228-288)\ \text{Å} \tag{31}$$

or

$$r_1 = (2-3)a^* \tag{32}$$

This value is the same as the value which was assumed in Ref. 39 for this model. For N larger than $N_{\max}$, it seems that some clusters are formed because the decrease in negative magnetoresistance is slower than the exponential decrease of N_m. A similar curve for the negative magnetoresistance of Ge is given in Ref. 39.

The M-NM transition occurs at the impurity concentration at which the Hall coefficient and resistivity at low temperatures become independent of temperature.[29] From Figs. 1 and 2 we see that for undoped and n-type samples, the M-NM transition occurs at a concentration between 3.3×10^{16} cm^{-3} (sample 0) and 4.7×10^{16} cm^{-3} (sample 1) which corresponds with $K \simeq 0.3$ to $N_c = (5.7\pm0.7)\times10^{16}$ cm^{-3}. This concentration is higher than $N_c = 2.3\times10^{16}$ cm^{-3} which we obtain from Mott's criterion.[40]

As is shown by Fritzsche,[41] and our data agrees (compare the curves for sample 3 and 3C in Fig. 2) with it, the M-NM transition shifts to higher carrier and majority impurity concentration with increasing degree of compensation. This is the cause of the observed shift of the M-NM transition of our undoped samples to a concentration higher than $N_c = 2.3\times10^{16}$ cm^{-3}, since these samples contain an appreciable degree of compensation (see Table V). As mentioned earlier in this section, the maximum of negative magnetoresistance occurs at a carrier concentration between 1×10^{16} cm^{-3} and 2×10^{16} cm^{-3}. This is close to the concentration corresponding to M-NM transition in undoped n-type GaAs. Hence, it seems that these two phenomena are related. Since the critical concentration N_c increases with compensation, one might be able to do a systematic study of the effect of compensation on the position of the maximum of the negative magnetoresistance and see whether these two phenomena are indeed related.

Figure 13 shows the carrier-density dependence of the carrier mobilities at 300 K in the conduction band and of the Hall mobility of impurity conduction at 4.2 K on the electron concentration at 300 K. It appears that the mobilities extrapolate to the same value near $n = 5\times10^{17}$ cm^{-3}. Above this concentration we believe the impurity band has merged with the conduction band. The decrease of the activation energies of undoped samples (see Table V) with increasing carrier concentration gives a similar indication. The peak of the Hall coefficient in Fig. 2 is shrinking as the carrier density increases and becomes very small for sample No. 5 which has carrier density of about 3.7×10^{17} cm^{-3}. This shows that $b = \mu_c/\mu_i$ is decreasing to

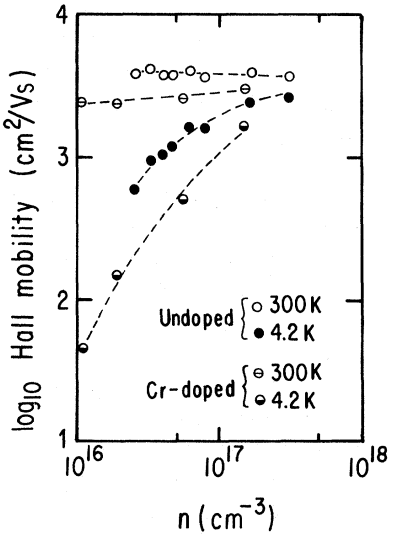

FIG. 13. Hall mobility as a function of the room-temperature carrier density of the samples listed in Tables III and IV.

unity [see Eq. (17)] as carrier density increases and becomes close to one for sample No. 5. This is again an indication that the bands merge at a carrier density near $n = 5 \times 10^{17}$ cm^{-3}. So we expect that the true metallic state in n-type GaAs starts at carrier density of about 5×10^{17} cm^{-3}. However, the presence of a small negative magnetoresistance above $n = 5 \times 10^{17}$ cm^{-3} suggests that some localized spins are still present in this true metallic region. This may be caused by some regions having a lower impurity concentration as a result of the random impurity distribution.

VI. SUMMARY AND CONCLUSIONS

Neutron transmutation doping is a well-controlled and reproducible method for introducing shallow donors into GaAs crystals. This doping method is approximately 1000 times more efficient in GaAs than in Si because of the higher abundances and neutron-capture cross sections of transmutable isotopes in GaAs. Moreover, the longest half-life encountered in the nuclear reactions in GaAs is only 26 h compared to 14.3 d in Si. Hence, the induced radioactivity decays to an acceptable low level for handling in a shorter time in GaAs than in Si. In epitaxially grown GaAs of high purity, the recoil and radiation damage associated with transmutation doping can be removed by annealing at about 600 °C, which is below the critical temperature for As effusion. Hence, no Si_3N_4 encapsulation is needed. In contrast, annealing near 800 °C is required to remove the damage associated with doping by ion implanation.

We found that such high annealing temperatures are also needed after transmutation doping of melt-grown GaAs crystals which were initially undoped or Cr doped. In contrast to epitaxially-grown GaAs, these crystals contain a high concentration of impurities and defects which can trap and bind either the transmuted atoms or the radiation (and recoil) defects and thus give cause for the higher annealing temperature.

After annealing we find that most transmuted Ge atoms are on Ga sites and most transmuted Se atoms are on As sites, giving rise to shallow donors. The measured concentrations of added donors for various neutron fluences agree well with the values deduced from the known abundances and neutron-capture cross sections of the transmutable isotopes. Our data on Cr-doped samples are less conclusive in this respect because they contained a high degree of compensation which prevented a reliable determination of the donor concentration added by transmutation doping.

For the epitaxial GaAs sample the donor and acceptor concentrations N_D and N_A could be determined by two independent methods. The analysis of the temperature dependence of the carrier concentration n in the conduction band yielded N_D and N_A values which were somewhat smaller than the values obtained by analyzing the temperature dependence of the mobility. We believe that the N_D and N_A values obtained from the T dependence of n represent the concentration of shallow donors and acceptors which are relevant for comparison with the transmutation doping theory. The additional ionized impurities revealed by the mobility analysis are most likely deep-lying impurity or defect centers which do not affect the temperature dependence of the carrier concentrations.

The transmutation-doped epitaxial GaAs sample was nonmetallic and showed a transition from band conduction above 4.2 K to impurity conduction below 4.2 K. Its magnetoresistance $\Delta\rho/\rho$ was positive at all temperatures. The value of $\Delta\rho/\rho$ peaked at 50 K, which corresponds to the temperature of maximum electron mobility in the conduction band, as well as at 4.2 K where band conduction and impurity conduction have equal magnitude. Below 4.2 K the magnetic field dependence of the resistivity agrees well with the theory of impurity conduction as modified by Shklovskii.[36,37]

After transmutation doping, our undoped as well as some of our Cr-doped melt-grown GaAs crystals were metallic, which means that R and ρ were temperature independent at the lowest temperatures. The magnetoresistance of the melt-grown samples was negative at low temperatures and increased in magnitude with decreasing temperature. This is in accordance with the theory of scattering of charge carriers from localized spins partially aligned in the magnetic field.[42]

A compilation of data from various authors and obtained by us revealed that the low-temperature magnetoresistance changes from positive to negative as the room-temperature carrier concentration n_0 is increased. The transition occurs near $n_0 = 2 \times 10^{15}$ cm^{-3} which is on the nonmetallic side of the nonmetal-metal transition. The negative magnetoresistance reaches a maximum value near $n_0 = 10^{16}$ cm^{-3} and then decreases with increasing n_0. It disappears when n_0 approaches 5×10^{17} cm^{-3}, which is the range of the so-called true metallic state which is characterized by the

absence of a Hall-effect maximum at higher temperatures.

We found that the nonmetal-metal transition occurs near $N_c = 5.7 \times 10^{16}$ cm^{-3} which is higher than the critical concentration $N_c = 2.3 \times 10^{16}$ cm^{-3} calculated from Mott's criterion[40] for this transition. We attribute this observation to the fact that our samples contain an appreciable degree of compensation. On the basis of physical arguments as well as experimental evidence, Fritzsche[41] pointed out that the critical concentration N_c increases with compensation.

Our observation that the maximum of the negative magnetoresistance and the nonmetal-metal transition occurring at close carrier concentrations n_0 suggests that these two phenomena are related. In summary, we find that transmutation doping is an alternative method of introducing a desired concentration of shallow donors into GaAs crystals for modifying their electronic properties. The inconvenience of this process compared to conventional doping methods may be offset by the possibility of irradiating larger quantities of material at one time.

ACKNOWLEDGMENTS

The author wishes to thank Dr. Jon M. Meese of the University of Missouri at Columbia for his help with the irradiation process and Professor C. M. Wolfe for supplying the epitaxial sample. Most of all, the author is deeply indebted to his thesis advisor, Professor H. Fritzsche, for his guidance and encouragement. This work was supported by the Air Force Office of Scientific Research under Contract No. AFOSR 80-0231; it is submitted to the Department of Physics, the University of Chicago, in partial fulfillment of the requirement for the Ph.D. degree.

[1] J. W. Cleland, K. Lark-Horovitz, and C. Pigg, Phys. Rev. 78, 814 (1950).
[2] H. Fritzsche and M. Cuevas, Phys. Rev. 119, 1238 (1960).
[3] M. Cuevas, Phys. Rev. 164, 1021 (1967).
[4] S. Golin, Phys. Rev. 132, 178 (1963).
[5] A. Kuehnel, H. Siethoff, and G. Landwehr, Phys. Status Solidi A 29, 387 (1975).
[6] F. Kuchar, E. Fantner, and G. Bauer, Phys. Status Solidi A 24, 513 (1974).
[7] Sh. M. Mirianashvili and D. I. Nanobashvili, Fiz. Tekh. Poluprovodn. 4, 1879 (1970) [Sov. Phys.—Semicond. 4, 1612 (1971)].
[8] M. A. Vesaghi and H. Fritzsche, in *Neutron Transmutation Doped Silicon,* edited by Jens Gulberg (Plenum, 1981), p. 487.
[9] R. Weast, *Handbook of Chemistry and Physics,* 58th ed. (Chemical Rubber Co., CRC Florida, 1977), pp. B-282, B284.
[10] *Neutron Cross Sections,* Vol. I of *Resonance Parameters,* edited by S. F. Mughabghab and G. I. Garber (Brookhaven Natl. Lab. Publications, Upton, New York, 1973), pp. B69, B70, B78.
[11] L. W. Aukerman, P. W. Davis, R. D. Graft, and T. S. Shilliday, J. Appl. Phys. 34, 3590 (1963).
[12] *Reactors Physics Constants,* 2nd ed. (U. S. Atomic Energy Commission, Div. of Techn. Information, Washington D. C., 1963), p. 631.
[13] R. Bauerlein, Z. Naturforsch. 14A, 1069 (1959); Z. Phys. 176, 498 (1963).
[14] Kindly supplied to us by Professor C. M. Wolfe of Washington University, St. Louis.
[15] E. Munoz, W. L. Snyder, and J. L. Moll, Appl. Phys. Lett. 16, 262 (1970).
[16] T. S. Blakmore, *Solid State Physics,* 2nd ed. (Saunders, Philadelphia, 1974), p. 340.
[17] O. V. Emelyanenko, T. S. Lagunova, and D. N. Nasledov, Fiz. Tverd. Tela 3, 198 (1961) [Sov. Phys.—Solid State 3, 144 (1961)].
[18] D. J. Oliver, Phys. Rev. 127, 1045 (1962).
[19] J. F. Woods and C. Y. Chen, Phys. Rev. 135A, 1462 (1964).
[20] O. V. Emelyanenko, T. S. Lagunova, D. N. Nasledov, and G. N. Talalakin, Fiz. Tverd. Tela 7, 1315 (1965) [Sov. Phys.—Solid State 7, 1063 (1965)].
[21] O. V. Emelyanenko, D. N. Nasledov, and N. A. Urmanov, Phys. Status Solidi 32, K175 (1969).
[22] Kh. I. Amirkhanov, R. I. Bashirov, and A. Yu. Mollaev, Fiz. Tverd. Tela 13, 849 (1971) [Sov. Phys.—Solid State 13, 701 (1971)].
[23] B. M. Vol., E. I. Zavaritskaya, I. D. Voronova, and N. V. Rozhdestrenskaya, Fiz. Tekh. Poluprovodn. 5, 943 (1971) [Sov. Phys.—Semicond. 5, 829 (1971)].
[24] V. M. Guslikov, O.V. Emelyanenko, D. N. Nasledov, D. D. Nedeoglo, and I. N. Timchenko, Fiz. Tekh. Poluprovodn. 7, 1785 (1973) [Sov. Phys.—Semicond. 7, 1191 (1974)].
[25] H. Fritzsche, J. Phys. Chem. Solids 6, 69 (1958).
[26] R. J. Sladek, J. Phys. Chem. Solids 5, 157 (1958).
[27] C. S. Hung, Phys. Rev. 79, 727 (1950).
[28] A. C. Beer, M. N. Chase, and P. F. Choquard, Helv. Phys. Acta 28, 529 (1955).

[29]H. Fritzsche, in *Proceedings of the Nineteenth Scottish Universities Summer School in Physics, 1978,* edited by L. R. Friedman and D. P. Tunstall (SUSSP Publications, Department of Physics, University of Edinburgh, 1978), p. 193.
[30]L. Halbo and J. Sladek, Phys. Rev. 173, 794 (1968).
[31]H. Kahlert and G. Landwehr, Z. Phys. B 24, 361 (1976).
[32]G. E. Stillman, C. M. Wolfe, and J. O. Dimmock, J. Phys. Chem. Solids 31, 1199 (1970).
[33]C. M. Wolfe, G. E. Stillman, and W. T. Lindley, J. Appl. Phys. 41, 3088 (1970). There are some printing mistakes in the equation of ionized impurity relaxation time of this publication; the correct form is

$$1/\tau_{II}(x) = 1.207\,63[(2N_A+n)/\epsilon_0^2] \times (m^*/m)^{-1/2}T^{-3/2}gx^{-3/2}\,.$$

[34]C. M. Wolfe, G. E. Stillman, and J. P. Dimmock, J. Appl. Phys. 41, 504 (1970).
[35]E. I. Zavaritskaya, I. D. Voronova, and N. V. Rozhdestvenskaya, Fiz. Tekh. Poluprovodn. 6, 1945 (1972) [Sov. Phys.—Semicond. 6, 1668 (1973)].
[36]B. I. Shklovskii, Fiz. Tekh. Poluprovodn. 6, 1197 (1972) [Sov. Phys.—Semicond. 6, 1053 (1973)].
[37]B. I. Shklovskii, Fiz. Tekh. Poluprovodn. 8, 416 (1974) [Sov. Phys.—Semicond. 8, 268 (1974)].
[38]V. H. Schonwald, Z. Naturforsch. 19A, 1276 (1964).
[39]Yu. V. Shmatrsev, E. F. Shender, and T. A. Polyanskaya, Fiz. Tekh. Poluprovodn. 4, 2311 (1970) [Sov. Phys.—Semicond. 4, 1990 (1971)].
[40]N. F. Mott, Proc. Phys. Soc. London 62, 416 (1949); Philos. Mag. 6, 287 (1961); Adv. Phys. 16, 49 (1967).
[41]H. Fritzsche, Philos. Mag. B 42, 835 (1980).
[42]Toyozawa, J. Phys. Soc. Jpn. 17, 986 (1962).